

Thermal Diffusivity Measurement of Two-Layer Optical Thin-Film Systems Using Photoacoustic Effect¹

K. U. Kwon,² M. H. Choi,² S. W. Kim,^{2,4} S. H. Hahn,² D. J. Seong,³
J. C. Kim,³ and S. H. Lee³

In this study, we designed and developed two-layer antireflection (AR) optical coating samples on glass substrates, using different evaporation conditions of coating rates and substrate temperatures for two dielectric materials, MgF₂ and ZnS, with different refractive indices. The through-plane thermal diffusivity of these systems was measured using the photoacoustic effect. The optical thicknesses of MgF₂ and ZnS layers were fixed at $5\lambda/4$ ($\lambda = 514.5$ nm) and λ , respectively, and the thermal diffusivities of the samples were obtained from the measured amplitude of the photoacoustic signals by changing the chopping frequency of the Ar⁺ laser beam. The results demonstrated that the thermal diffusivity of the sample fabricated under the conditions of $10 \text{ \AA} \cdot \text{s}^{-1}$ and 150°C had the maximum value and that the results were directly related to the microstructure of the film system.

KEY WORDS: antireflection coating; parameter estimation; photoacoustic effect; thermal diffusivity; through-plane.

1. INTRODUCTION

In the development of high-power lasers such as carbon dioxide and Nd:YAG lasers used in the cutting and welding of metal plates and the Nd:glass laser used for laser fusion, the required mirrors must be heat

¹ Paper presented at the Fifth Asian Thermophysical Properties Conference, August 30–September 2, 1998, Seoul, Korea.

² Department of Physics, University of Ulsan, Ulsan 680-749, Korea.

³ Temperature Group, Korea Research Institute of Standards and Science, Taejeon 305-600, Korea.

⁴ To whom correspondence should be addressed.

resistant and effectively cooled. Thus, it is important to identify multilayer optical thin-film systems for which the thermal diffusivity is large.

The photoacoustic (PA) effect has been proven to be an effective and sensitive tool for studying optical and thermal properties of solids, liquids, gases, and films [1]. By using the PA technique, one can obtain quantitative information on sample properties such as the thermal diffusivity, the optical absorption coefficient, or the depth profile of a thin-film system [2].

When the films are thermally thin, the reflected thermal waves from their interfaces interfere [3, 4], and therefore the PA effect in multilayer thin-film systems becomes very complicated. Until now, many researchers have studied PA effects in multilayer thin films only theoretically or, if experimentally, only in limited cases [4–6]. Thus, it is not easy to apply this effect to real situations.

In this study, to investigate the influence of the microstructure of optical thin films on the through-plane thermal diffusivity, we prepared several kinds of two-layer antireflection (AR) optical coating samples under different evaporation conditions such as coating rate and substrate temperature. Then we measured the thermal diffusivity by using the PA effect through the parameter estimation technique. In the theoretical treatment, we used an expression for the temperature of the front surface of a five-layered system [7] which includes the substrate, a two-layer thin-film system, an absorbing layer such as liquid graphite, and air.

2. EXPRESSIONS FOR AMPLITUDE OF PA SIGNAL

In a multilayer film system, the thermal wave is reflected from the interfaces and undergoes interference, and thus the boundary conditions become very complicated.

A schematic of the five-layer system is shown in Fig. 1. The five-layered sample, consisting of a backing material (substrate) 0 and the three successive layers (1, 2, 3), is heated by a modulated heating beam. An additional medium, 4, such as air is in contact with the surface absorbing layer 3. The backing material and surrounding material are assumed to be thermally thick. By applying the Rosencwaig–Gersho (RG) theory, one obtains the following expression for the surface temperature $T_s(x=0, t)$ [7]:

$$T_s(x=0, t) = E_3(t) \frac{f_3 + h_3}{f_3 + f_4} \frac{A_3 W_3 (1 - e^{-b_3}) - B_3 (e^{-u_3} - e^{-b_3})}{A_3 + r_{3,4} B_3 e^{-u_3}} \quad (1)$$

where

$$f_i = \sigma_i k_i \tag{2}$$

$$u_i = 2d_i \sigma_i \tag{3}$$

$$r_{i,i+1} = (f_i - f_{i+1}) / (f_i + f_{i+1}) \tag{4}$$

$$h_i = \beta_i k_i \tag{5}$$

$$b_i = d_i (\sigma_i + \beta_i) \tag{6}$$

$$W_i = (h_i - f_i) / (h_i + f_i) \tag{7}$$

$$E_i(t) = h_i / (h_i^2 - f_i^2) Q(t) \tag{8}$$

$$A_3 = 1 + r_{0,1} r_{1,2} e^{-u_1} + (r_{1,2} + r_{0,1} e^{-u_1}) r_{2,3} e^{-u_2} \tag{9}$$

$$B_3 = (1 + r_{0,1} r_{1,2} e^{-u_1}) r_{2,3} + (r_{1,2} + r_{0,1} e^{-u_1}) e^{-u_2} \tag{10}$$

The $r_{i,i+1}$ in Eqs. (9) and (10) are the reflection coefficients of thermal waves from the interfaces between the i th and $(i+1)$ th layers. If the properties of the individual films including the thermal diffusivity are already known, the temperature of the front surface $T_s(x=0, t)$, which depends on the modulation frequency, can be calculated by using Eq. (1). The $T_s(x=0, t)$ can be assumed to be proportional to the amplitude of the PA signal from the multilayer sample [2].

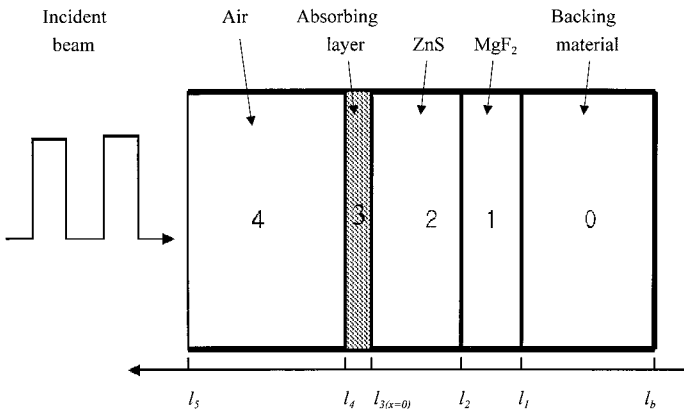


Fig. 1. Cross-sectional view of five-layer model.

3. PARAMETER ESTIMATION

Parameter estimation (PE) is a powerful technique that can use all the available data points and provide a statistical means to analyze an experiment [8]. Because there are so many unknown parameters in Eq. (1), we cannot apply the PE technique directly to this equation. Under the assumption of proportionality between $T_s(x=0, t)$ and the amplitude of the PA signal, we can reduce the number of unknown parameters to three by substitution of the $T_s(x=0, t)$ into the following equation for A , which was derived from RG theory [9] to express the amplitude variation of the PA signal for the case of a one-layer film deposited on a substrate (backing material):

$$A = \frac{A_0}{2Y^2} \left[\frac{\left(\begin{array}{c} \{(1+g)e^Y + (1-g)e^{-Y}\}^2 \cos^2 Y \\ + \{(1+g)e^Y - (1-g)e^{-Y}\}^2 \sin^2 Y \end{array} \right)}{\left(\begin{array}{c} \{(1+g)e^Y - (1-g)e^{-Y}\}^2 \cos^2 Y + \{(1+g)e^Y \\ + (1-g)e^{-Y}\}^2 \sin^2 Y \end{array} \right)} \right]^{1/2} \quad (11)$$

where A_0 is a constant amplitude, $g = \varepsilon_b/\varepsilon_s$ (subscript b indicates backing material, subscript s indicates single-layer film), and $Y = \sqrt{\pi f/f_c}$, with $f_c = \alpha_i/d_i^2$ a characteristic frequency.

The PE procedure was used to find optimum values for the three parameters of A_0 , Y , and g from Eq. (11). From the value of Y , the characteristic frequency f_c can be obtained and the thermal diffusivity can be calculated from $f_c = \alpha_i/d_i^2$ for a known thickness. A nonlinear PE algorithm NL2SOL developed by Dennis et al. [10, 11] was used in this work.

4. EXPERIMENTS

4.1. Sample Preparation

We prepared AR-coating samples by resistive heating evaporation at different evaporation conditions of substrate temperature (50, 100, 150, 200°C) and coating rate (10, 20 Å·s⁻¹), using two dielectric materials of MgF₂ and ZnS. The reference wavelength λ is 514.5 nm and the designed film structure is air/(ZnS, λ)/(MgF₂, $5\lambda/4$)/substrate, where λ and $5\lambda/4$ are the optical thicknesses of ZnS and MgF₂, respectively.

4.2. Apparatus

The experimental setup is shown in Fig. 2. The heating beam from an Ar⁺ laser is absorbed by the sample placed in the PA cell. The beam is

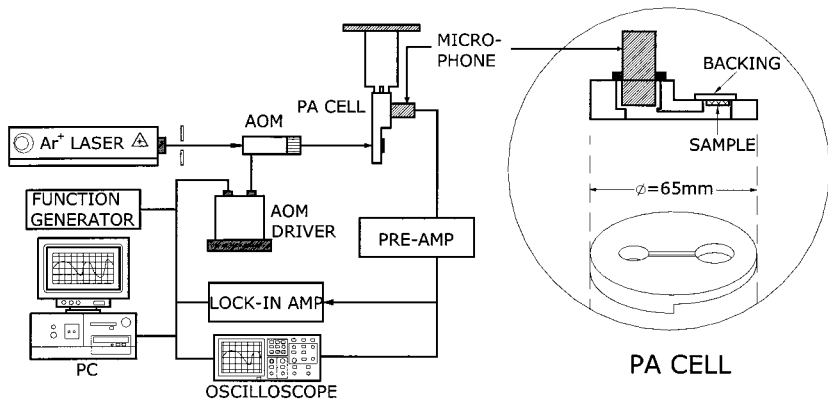


Fig. 2. Schematic diagram of the experimental setup and the design of a photoacoustic cell.

modulated by an acoustooptic modulator (AOM) whose modulation frequency can be varied from a few Hz to a few MHz. The beam size on the sample surface is fixed by a condensing lens and iris to be 10 mm. For the detection and amplification of the PA signal, we used a 1.3-cm microphone (B&K 2639) whose sensitivity is $40 \text{ mV} \cdot \text{Pa}^{-1}$ and preamplifier, respectively. A dual-phase lock-in amplifier (EG&G 5110) is used to analyze the phase and amplitude of the signal. Figure 2 also shows the design of the PA cell. To minimize the stray effect and other background noises, the cell was made of plexiglass, whose absorption is negligible. There are two chambers in the cell, one for the sample and the other for the microphone. The two chambers are connected by a narrow channel. The amplitude of the PA signal was measured by changing the frequency from a few Hz to tens of kHz.

5. RESULTS AND DISCUSSION

First, we measured the amplitude variation of each single-layer sample (MgF_2 , ZnS) and two-layer samples prepared at different evaporation conditions by changing the modulation frequency. Figure 3 shows the result for a typical case. It shows that, as the modulation frequency increases, the amplitude of the PA signal decreases and the signal amplitude from the two-layer sample is larger than that from the single layers over the complete frequency range.

The second and third columns of Table I give the measured thermal diffusivities of single-layered MgF_2 and ZnS , respectively, found with the PE procedure using Eq. (11). The experiments were performed five times for each sample, and the error boundary was obtained from this result. The

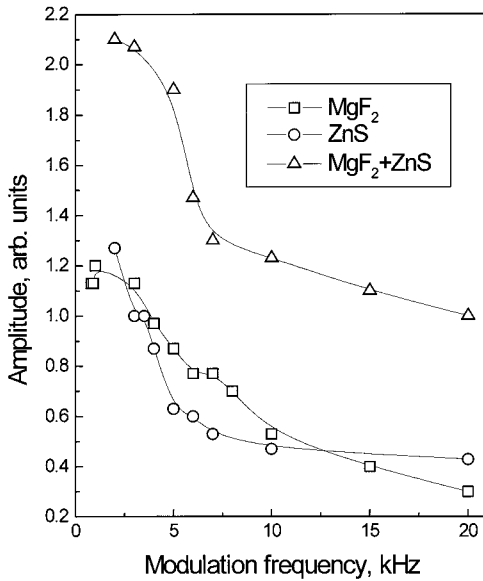


Fig. 3. Amplitude of PA signal as a function of modulation frequency (evaporation rate, $10 \text{ \AA} \cdot \text{s}^{-1}$).

reliability of this measuring method and apparatus has been verified by using five kinds of metal samples [9]. Although the errors contained in d_i and f_c can influence the accuracy of α_i , they can be neglected within the obtained error boundaries because α_i is proportional to d_i^2 and f_c is very stable over a frequency range of several kHz.

The thermal diffusivity of MgF_2 was always larger than that of ZnS . This was assumed to be caused by the relation of the thermal diffusivity to

Table I. Thermal Diffusivity ($10^{-5} \text{ cm}^2 \cdot \text{s}^{-1}$) of Single-Layer and Two-Layer Thin-Film Systems Evaporated on Substrates at Different Temperatures^a

Temp. ($^{\circ}\text{C}$)	Single-layer film		Two-layer film
	MgF_2	ZnS	
50	4.98 ± 0.13	1.78 ± 0.05	3.79 ± 0.10
100	6.47 ± 0.15	1.39 ± 0.03	4.64 ± 0.11
150	5.45 ± 0.13	1.31 ± 0.03	9.72 ± 0.23
200	4.64 ± 0.29	1.30 ± 0.08	8.37 ± 0.52

^a Evaporation rate, $10 \text{ \AA} \cdot \text{s}^{-1}$.

the geometrical thickness of such very thin films [12]. Because the refractive indices of ZnS and MgF₂ are 2.30 and 1.35 at 514.5 nm, respectively [12], the geometrical thickness (optical thickness divided by refractive index) of MgF₂ is about two times larger than that of ZnS. As the temperature of the substrate increases, the thermal diffusivity of ZnS slightly decreases and that of MgF₂ fluctuates. The reason for this is not clear and needs more investigation.

Next, the measured values found for the single layers by PE and other values of single layers were substituted into Eq. (1) through Eqs. (2) to (10). Finally, the thermal diffusivity of the two-layer sample was obtained. The fourth column of Table I gives the thermal diffusivity of two-layer films. Figure 4 shows the results for a two-layer sample (fourth column of Table I). As the substrate temperature increases, the thermal diffusivity also increases and becomes a maximum when the substrate temperature is 150°C, and, after that, it slightly decreases. A possible explanation is that, as the temperature of the substrate increases, the surface mobility of vapor molecules also increases generally and is packed more densely, and the diameter of the columnar microstructure increases [13] (Fig. 5).

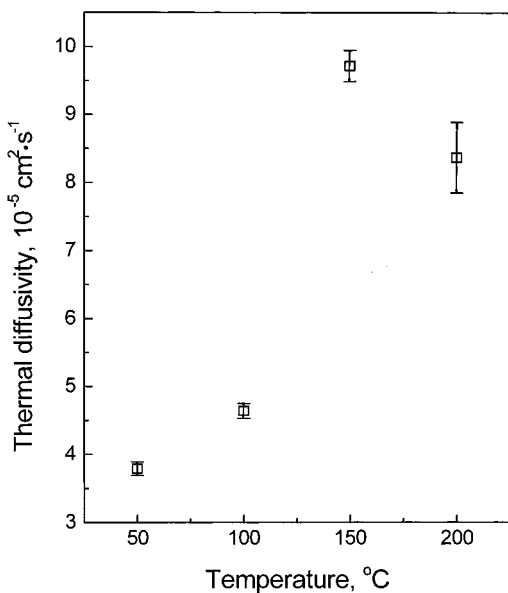


Fig. 4. Thermal diffusivity of two-layer thin-film systems as a function of substrate temperature (evaporation rate, 10 Å·s⁻¹).

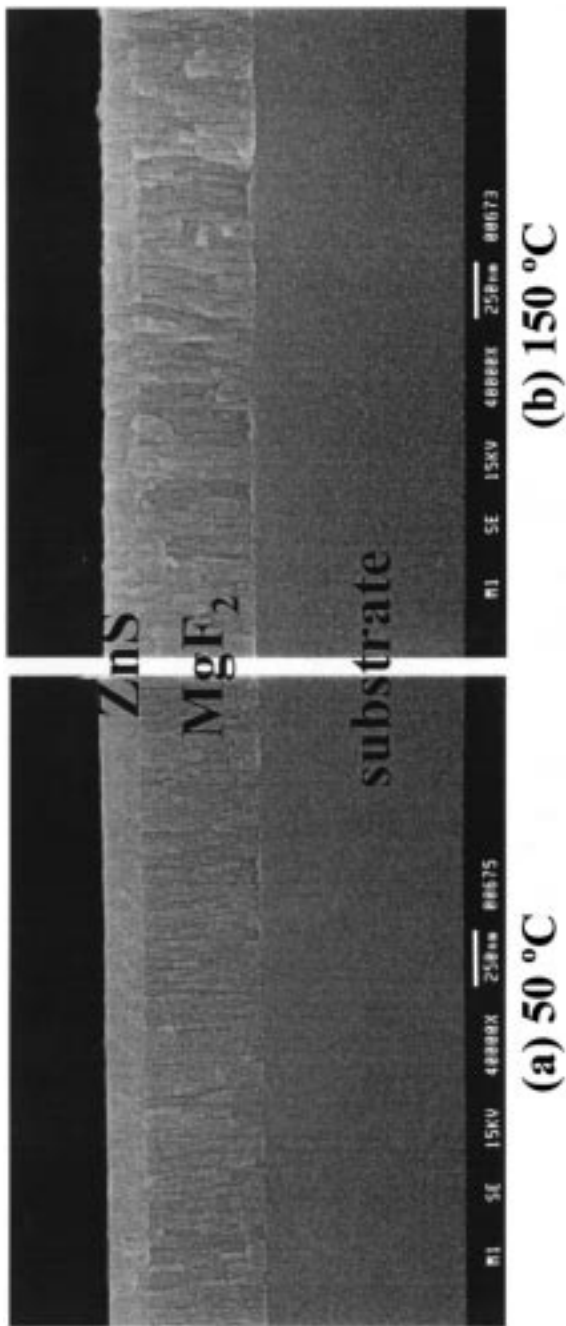


Fig. 5. Cross-sectional micrographs of a two-layer thin film at different substrate temperatures (evaporation rate, $10 \text{ \AA} \cdot \text{s}^{-1}$). (a) Substrate temperature, 50°C , (b) substrate temperature, 100°C .

Table II. Thermal Diffusivity ($10^{-5} \text{ cm}^2 \cdot \text{s}^{-1}$) of Single-Layer and Two-Layer Thin-Film Systems Coated at Different Evaporation Rates^a

Coating rate ($\text{\AA} \cdot \text{s}^{-1}$)	Single-layer film		Two-layer film
	MgF ₂	ZnS	
10	5.45 ± 0.13	1.31 ± 0.03	9.72 ± 0.23
20	4.38 ± 0.20	1.37 ± 0.06	8.14 ± 0.37

^a Substrate temperature, 150°C.

Table II shows the results from the samples prepared for a fixed substrate temperature of 150°C and at different coating rates. The case for a coating rate of $10 \text{ \AA} \cdot \text{s}^{-1}$ shows larger thermal diffusivities than that for $20 \text{ \AA} \cdot \text{s}^{-1}$. This was also caused by the microstructure of the deposited film layers. Although optimum coating rates for these dielectric materials are about 10 to $30 \text{ \AA} \cdot \text{s}^{-1}$ [14], the coating rate must not be too high, otherwise relaxation processes of already deposited particles may be inhibited and clusters may also form in the vapor phase.

6. CONCLUSIONS

The thermal diffusivities of a two-layer optical film system have been measured by using a five-layer model which considers the reflection of thermal waves from the interfaces. We obtain the following results:

1. The thermal diffusivity value is of the order of $10^{-5} \text{ cm}^2 \cdot \text{s}^{-1}$.
2. As the substrate temperature increases, the thermal diffusivity also increases and becomes a maximum when the substrate temperature is 150°C.
3. The thermal diffusivity for a coating rate of $10 \text{ \AA} \cdot \text{s}^{-1}$ is larger than that for $20 \text{ \AA} \cdot \text{s}^{-1}$.
4. These results can be extended to high-reflectance, multilayer optical coating systems.

NOMENCLATURE

c_i	isobaric specific heat
$d_i = l_{i+1} - l_i$	thickness of medium i
k_i	thermal conductivity
$Q(t)$	heat flux

$$\alpha_i$$

$$\beta_i$$

$$\varepsilon_i = k_i / \sqrt{\alpha_i}$$

$$\sigma_i = (1 + j)(\omega \rho_i c_i / 2k_i)^{1/2} \text{ with } j = \sqrt{-1}$$

thermal diffusivity
 optical absorption coefficient
 thermal effusivity

ACKNOWLEDGMENT

This work has been supported by the Korea Science and Engineering Foundation (Grant No. 976-0200-001-2) and was supported in part by the Korea Science and Engineering Foundation through the Research Center for Machine Parts and Materials Processing at the University of Ulsan.

REFERENCES

1. A. Philip, P. Radhakrishnan, V. P. N. Nampoori, and C. P. G. Vallabhan, *J. Appl. Phys. D* **26**:836 (1993).
2. A. Rosenzweig, *Photoacoustics and Photoacoustic Spectroscopy* (Wiley, New York, 1980), Chap. 9.
3. F. A. McDonald, *Am. J. Phys.* **48**:41 (1980).
4. C. A. Bennett, Jr., and R. R. Patty, *Appl. Opt.* **21**:49 (1982).
5. Y. Fujii, A. Moritani, and J. Nakai, *Jpn. J. Appl. Phys.* **20**:361 (1981).
6. M. Morita, *Jpn. J. Appl. Phys.* **20**:835 (1981).
7. J. Baumann and R. Tilgner, *J. Appl. Phys.* **58**:1982 (1985).
8. J. V. Beck and K. J. Arnold, *Parameter Estimation* (Wiley, New York, 1977), pp. 117-129.
9. S. W. Kim, J. Lee, and R. E. Taylor, *Int. J. Thermophys.* **12**:1063 (1991).
10. J. E. Dennis, Jr., D. M. Gay, and R. E. Welsch, *Trans. Math. Software* **7**:348 (1981).
11. J. E. Dennis, Jr., D. M. Gay, and R. E. Welsch, *Trans. Math. Software* **7**:369 (1981).
12. K. U. Kwon, M. H. Choi, S. W. Kim, S. H. Hahn, and J. T. Kim, *J. Opt. Soc. Korea* **9**:380 (1998).
13. K. H. Guenther, *Appl. Opt.* **23**:3806 (1984).
14. E. Welsch, H. G. Walther, and R. Wolf, *Thin Solid Films* **156**:1 (1988).